Fourier Analysis of Memristor Excited by Sinusoidal Signal

VIERA BIOLKOVÁ[1)], DALIBOR BIOLEK[2,3)], ZDENĚK KOLKA[1)]
Depts. of Radioelectronics [1)] and Microelectronics [2)], Brno University of Technology
Dept. of EE [3)], University of Defence Brno
CZECH REPUBLIC
dalibor.biolek@unob.cz http://user.unob.cz/biolek

Abstract: - The paper deals with the analysis of flux-controlled memristor which is described by its unambiguous charge-flux constitutive relation. The memristor is excited by ideal sinusoidal voltage source in order to sense its typical $i - v$ pinched hysteretic loop. Two equivalent schematics of the transformation of the exciting voltage into the current response are described. The first one is selected for the spectral analysis of the current. It is shown that the corresponding Fourier series contains only the sine terms. It confirms the fact that the pinched hysteretic loops of ideal memristors must be always odd-symmetrical.

Key-Words: -Memristor, constitutive relation, pinched hysteretic loop, spectral analysis, charge, flux

1 Introduction

The memristive systems, which are intensively studied particularly for their potential utilization in digital or analog memories, are characteristic by their typical pinched hysteretic loops (PHLs) [1]. These patterns, plotted in the current-voltage characteristics of these systems under their periodical excitation, belong to well-known fingerprints of the corresponding memory effects.

The above loops are important characteristics of memristive systems because they can be easily obtained via common measuring equipments. These loops can be of various shapes [2-6], as shown in the results published in several technical disciplines [7]. Some curves have the so-called odd symmetry, some of them do not. The original paper [8], in which the memristive systems are introduced, contains a note about two properties of PHLs of memristive system under sinusoidal excitation: "Double-valued Lissajous Figure Property", and "Symmetric Lissajous Figure Property". The paper [7] refers to possible cases when the PHL degenerates to a graph of single-valued function. It is also shown in [7] that, in contrast to classical memristor, the definition of general memristive system provides a lot of degrees of freedom, and thus the PHLs of such systems can significantly differ from the PHLs of the memristors.

The rules and fundamental limitations of the shapes of PHLs of classical memristors are not analyzed to a satisfactory degree in hitherto published papers. In [9-12] and other papers, examples of memristors with prescribed flux-charge constitutive relations (CRs) are only given which lead to odd-symmetrical PHLs. However, it is not mentioned if this property relates to the PHLs of all memristors with unambiguous CR. The analysis of a surface bounded by the PHL of "HP memristor" is given in [13]. As far as we know, a generalization to memristors with arbitrary CR has not been published so far. Based on the calculation of energies dissipated in the memristor during one repeating period of the exciting signal, the so-called "Quantitative measure of hysteresis" is introduced in [14]. However, such a quantity does not represent the surface within the PHL.

The shape of the PHL is determined by the pattern of the harmonic terms of voltage and current waveforms. Consequently, it is useful to deal with the Fourier analysis of these waveforms under the condition of periodical excitation of the memristor.

The following considerations will be focused on the time-invariant flux-controlled memristor, or memristor with the CR defined by unambiguous functional relationship between the flux φ (= cause) and charge q (= consequence) [15]

$$q = \hat{q}(\varphi)\,, \tag{1}$$

where $\hat{q}(\varphi)$ is the continuous and piecewise differentiable function, specified in [7]. These considerations can be easily extended to the charge-controlled memristor via the duality theorem [15].

The CR (1) is the basic characteristic of the memristor, expressing also the idea of memristor model in the sense of "Flux-dependent Ohm's law" [7]:

$$i = \frac{dq}{dt} = G_M(\varphi)v\,, \tag{2}$$

where

$$G_M(\varphi) = \frac{d\hat{q}(\varphi)}{d\varphi} \tag{3}$$

ISBN: 978-1-61804-055-8

is a flux-dependent memductance. This dependence of the memductance on the history of the evolution of memristor voltage is reflected in the ambiguous current-voltage response, represented by the steady-state PHL [7, 15].

Recently, general memristive systems, introduced in [8], have come to be referred to as memristors [7, 16]. For example, the Chapter "Unfolding the memristor" in [7] provides an extension of the equations of a classical memristor by other state variables and parameters in order to tweak the PHLs in a very general way. However, such generalized equations model the memristive system as in [1, 8].

To avoid any misunderstanding, note that this study deals with the memristor defined in the original work [15] as the fourth fundamental circuit element, i.e. by its CR (1). The memristor will be excited by ideal voltage source with the zero-valued DC component, with the waveform

$$v(t) = V \sin(\Omega t) \tag{4}$$

where V and Ω are the amplitude and the angular frequency, the latter being related to the repeating frequency F in Hertz and to the repeating period T in seconds according to the relations $\Omega = 2\pi F = 2\pi/T$.

2 Memristor with nonlinear CR excited by harmonic signal

Consider the flux-controlled memristor with nonlinear CR (1), excited by ideal voltage source with the waveform (4). The mechanism of generating the current flowing through the memristor can be described by means of the block diagram in Fig. 1.

However, this method is not useful for computer modeling of the memristor behavior since it contains the block of the time-domain differentiation, the well-known source of numerical problems, amplifying the numerical noise. That is why the block diagram in Fig. 2 is more suitable for the simulation. The current is not computed from the CR but from another equivalent characteristic, the memductance as a function of the flux (a similar characteristic is denoted in [7] "resistance vs. state map"). The current is then computed from the memristance and voltage via "flux-dependent Ohm's law".

It is easy to implement the memristor model in Fig. 2 in some of the commonly used simulation programs, and to utilize it for interesting experiments.

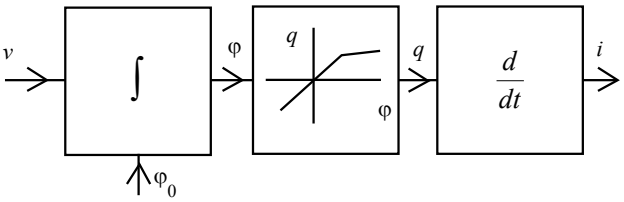

Fig. 1: Block diagram of the transformation of the terminal voltage of the flux-controlled memristor into current via CR.

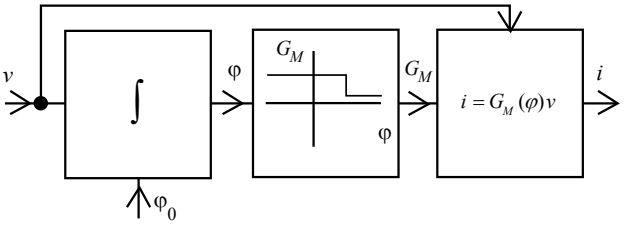

Fig. 2: Block diagram of the transformation of the terminal voltage of the flux-controlled memristor into current via the flux-dependent memductance.

For example, consider the CR (1) of the memristor in the form of the Taylor series

$$q = \sum_{k=1}^{\infty} g_k \varphi^k \,, \tag{5}$$

where g_k, k=1, 2, .. are real numbers. The series does not contain the absolute term, thus the CR graph will go through the origin of the q-φ coordinates.

Differentiation according to Eq. (3) yields the formula of the memductance:

$$G_M(\varphi) = \sum_{k=1}^{\infty} k g_k \varphi^{k-1} \,. \tag{6}$$

A listing of the PSPICE code for simulating the behavior of memristors with the CR (5), considering the first five terms of the Taylor expansion, is shown below.

```
*Model of flux-controlled memristor
*excited by sine-wave voltage source
*CR of the memristor is modeled via polynomial (5)
.param V 1 freq 10 omega {2*pi*fre} phi0 0;line 1
.param g1 1.5m g2 -9m g3 10 g4 -360 q5 3k ; line 2
Ein in 0 value={V*sin(omega*time)} ;line 3
Ephi phi 0 value={phi0+SDT(v(in))} ;line 4
Gm in 0 value={(g1+2*g2*v(phi)+3*g3*v(phi)**2+
+ 4*g4*v(phi)**3+5*g5*v(phi)**4)*v(in)} ; line 5
.tran 0 0.2 0 0.2m skipbp ;line 6
.probe ; line 7
.end
```

Choosing concrete values of the coefficients g_k, various types of CR, waveforms, and PHLs can be obtained.

ISBN: 978-1-61804-055-8

The amplitude and repeating frequency of the sine-wave voltage, and the initial value phi0 are defined on Line 1.

The coefficients of the Taylor series are given on Line 2.

The model of voltage source according to Eq. (4) is on Line 3.

The flux computation via time-domain integration of voltage by means of the SDT function is on Line 4.

Line 5 contains a model of controlled current source, simulating the memristor. The current value is computed via Ohm's law, with the memductance given by the series (6).

The transient analysis within a time interval of up to 0.2 seconds and with a maximum time step of 0.2 msec. is specified on Line 6.

Line 7 contains the command for running the graphical postprocessor PROBE.

It is obvious from Line 1 that the memristor being modeled is excited by the sinusoidal voltage with an amplitude of 1V and a repeating frequency of 10 Hz. The initial value of the flux is set to zero. Since the voltage has the sine form, the flux values are nonnegative, and the operating point will cross the CR curve only in the first quadrant, similar to the case in [7]. This condition can be modified via setting a nonzero value of phi0. The CR is tweaked by a pentad of g_k coefficients.

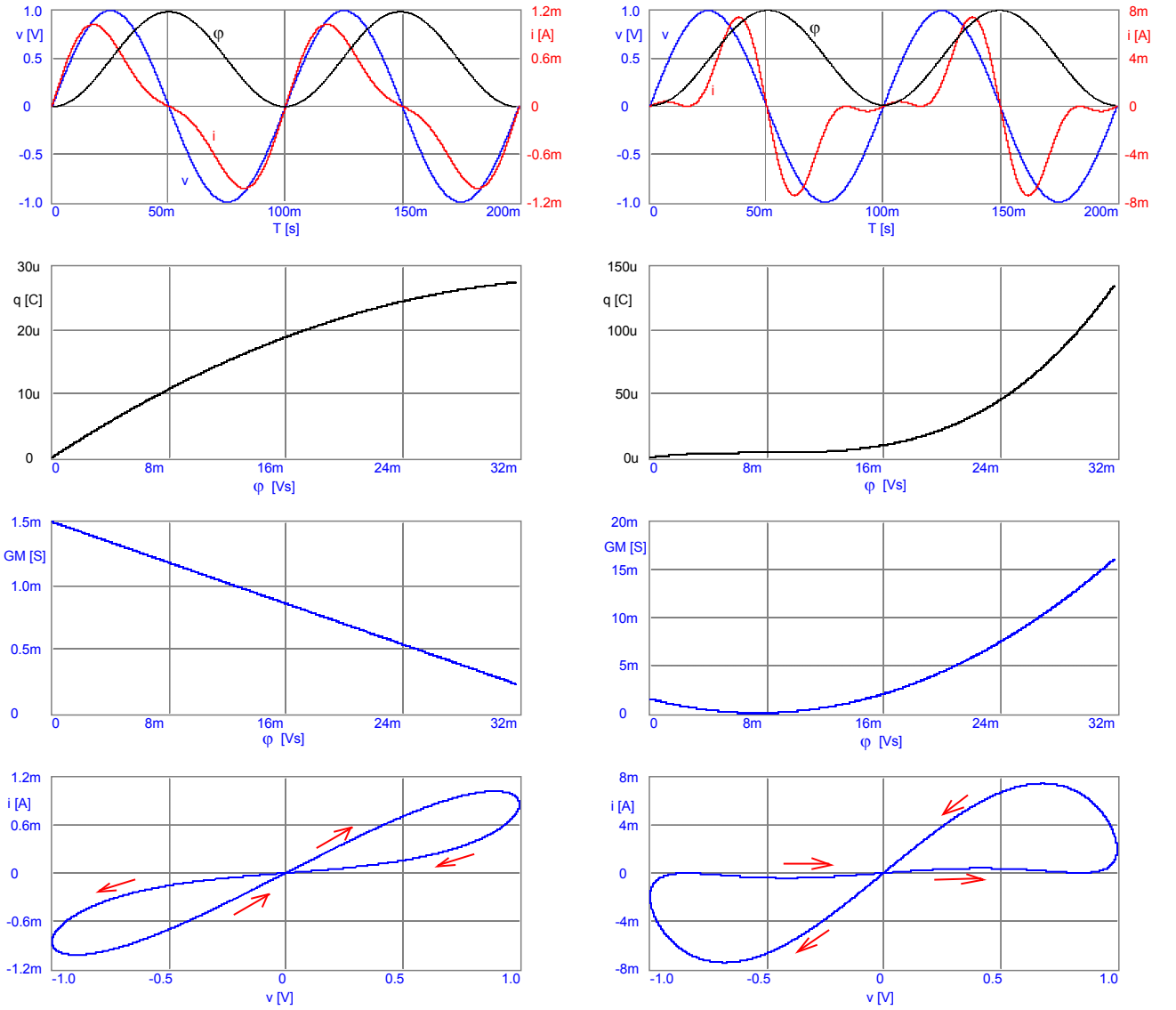

Fig. 3: Voltage and current waveforms, CR, memductance versus flux, *i-v* pinched hysteretic loops for the coefficients [g_1, g_2, g_3, g_4, g_5] (a) [1.5m, -20m, 0, 0, 0], (b) [1.5m, -0.2, 9, 0, 0]; flux (φ) waveforms vary from 0 to ca 32 mVs.

ISBN: 978-1-61804-055-8

3 Fourier analysis of memristor excited by sine-wave voltage

A detailed mechanism of generating the current floating through the memristor, excited by the sine-wave voltage source, is shown in Fig. 4. Three blocks are between the two signals (voltage and current), two of them being linear inertial (integrator and differentiator) and one nonlinear non-inertial (block modeling the CR). Passing the signal through these blocks causes linear and non-linear distortions with the well-known consequences in the time and frequency domains. Voltage-to-flux integration causes an amplitude modification and the formation of the DC component of the flux, which is dependent on the amplitude and frequency of the voltage waveform and also on the history of memristor behavior, which is represented by the initial flux φ_0. The integration also leads to a phase delay of the AC component of the flux by 90 degrees with respect to the exciting voltage. The flux is transformed into charge via nonlinear CR. The corresponding charge waveform is distorted by this transformation. The character of this distortion also depends on the DC component of the flux, which is influenced by the amplitude and frequency of the exciting voltage and by the memristor history. Since the nonlinear flux-charge transformation is noninertial, the harmonic components of the charge, generated by spreading the spectrum after passing the signal through the nonlinear system, are in phase with the AC component of the flux or, possibly, some of them can be shifted by 180 degrees (see the following analysis). The differentiation of the charge with respect to time yields a current that is free of the DC component. The differentiation causes the well-known linear distortion called pre-emphasis, and the initial phases of all harmonic

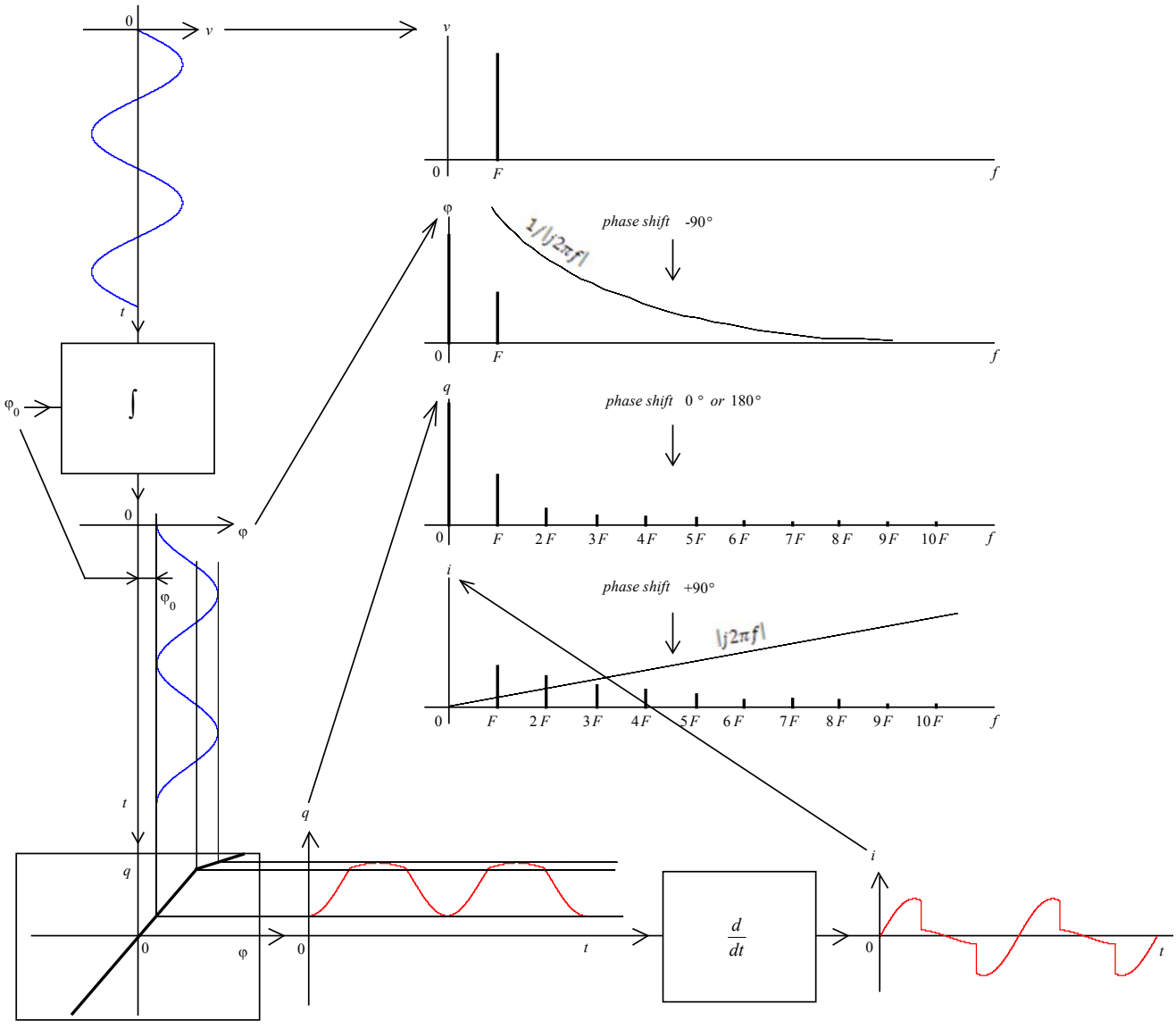

Fig. 4: Mechanism of memristor voltage-to-current conversion in time- and frequency-domains.

ISBN: 978-1-61804-055-8

components are increased by 90 degrees. As a result, the sine voltage, with its initial phase of -90 degrees, is converted via three blocks to a current consisting of harmonic components, each having the initial phase either -90 degrees or +90 degrees. Both voltage and current are thus described by odd functions of time, and the current-voltage pinched hysteretic loop must therefore be odd-symmetrical.

The above mechanism of voltage-to-current conversion from Fig. 4 can be described mathematically as follows.

The terminal voltage of the memristor (4) is transformed via integration into the flux:

$$\varphi(t) = \varphi_0 + \int_0^t v(\alpha)d\alpha = \varphi_0 + \frac{V}{\Omega} - \frac{V}{\Omega}\cos(\Omega t) \qquad (7)$$

where φ_0 is the initial flux at time 0.

The flux waveform can be divided into a DC part φ_{DC}, which depends on the initial condition φ_0 and on the amplitude-to-frequency ratio of the exciting voltage, and a harmonic component $\tilde{\varphi}(t)$ with the same frequency as that of the exciting voltage , and with the amplitude being the ratio of the amplitude and the frequency of the voltage waveform. The initial phase of this component is 90 degrees below the initial phase of the voltage. The DC component of the flux sets the operating point [φ_{OP} , q_{OP}] in the CR curve, see Fig. 5. Eq. (7) can be modified to the following form:

$$\varphi(t) = \varphi_{OP} + \tilde{\varphi}(t) = \varphi_{OP} - \Phi\cos(\Omega t) \qquad (8)$$

where

$$\varphi_{OP} = \varphi_0 + \frac{V}{\Omega},\ \Phi = \frac{V}{\Omega}. \qquad (9)$$

Similar to Eq. (8), the charge can be divided into DC and AC components:

$$q(t) = q_{OP} + \tilde{q}(t) \qquad (10)$$

Note that Eq. (5) represented the Taylor expansion of the CR near the origin of the coordinates (φ, q). An analogous expansion of the CR near the operating point [φ_{OP} , q_{OP}] is

$$\tilde{q} = \sum_{k=1}^{\infty} \tilde{g}_k \tilde{\varphi}^k . \qquad (11)$$

The coefficients of the Taylor series (11) and (5) are tied by the well-known transformation

$$\tilde{g}_k = \sum_{i=k}^{\infty} g_i \binom{i}{k} \varphi_{OP}^{i-k} . \qquad (12)$$

Substituting $\tilde{\varphi}$ from (8) to (11) and elaborated arrangements yield the Fourier series of $\tilde{q}(t)$:

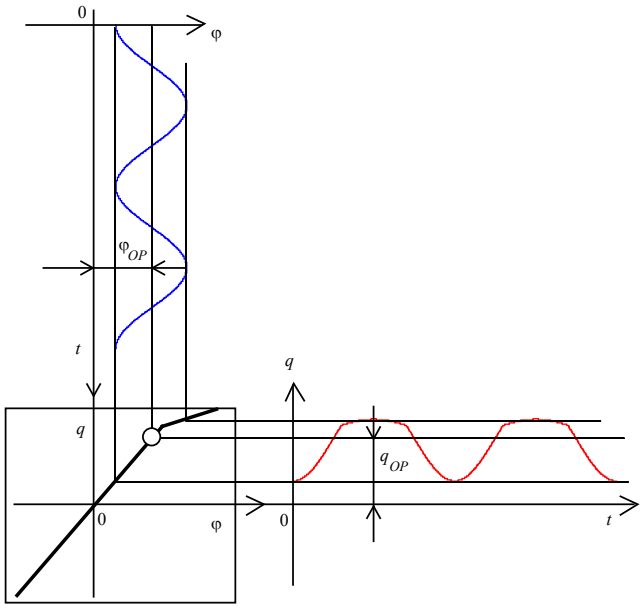

Fig. 5: Definition of the quantities φ_{OP} and q_{OP}.

$$\tilde{q}(t) = \sum_{m=0}^{\infty} \tilde{q}_m \cos(m\Omega t), \qquad (13)$$

where

$$\tilde{q}_0 = \sum_{i=1}^{\infty} (-1)^i \tilde{g}_i \Phi^i 2^{-i} \binom{i}{\frac{i}{2}}, \qquad (14)$$

$$\tilde{q}_m = \sum_{i=m}^{\infty} (-1)^i \tilde{g}_i \Phi^i 2^{1-i} \binom{i}{\frac{i-m}{2}},\ m > 0. \qquad (15)$$

Note that the binomial coefficient $\binom{n}{k}$ is zero if n, k are not integer numbers.

The memristor current is equal to derivative of the signal $\tilde{q}(t)$ with respect to time, or

$$i(t) = \sum_{m=0}^{\infty} (-\tilde{q}_m m\Omega)\sin(m\Omega t) . \qquad (16)$$

After rewriting

$$i(t) = \sum_{m=1}^{\infty} i_m \sin(m\Omega t), \qquad (17)$$

where

$$i_m = m\sum_{i=m}^{\infty} (-1)^{i+1} \tilde{g}_i \frac{V^i}{(2\Omega)^{i-1}} \binom{i}{\frac{i-m}{2}},\ m > 0. \qquad (18)$$

The following conclusions result from the above analysis:

The Fourier series of the meminductor current contains only sine-type components. The current as well as the voltage waveforms are thus odd functions of time. The corresponding hysteretic loop in the *i-v* coordinates must be “pinched” and odd-symmetric.

ISBN: 978-1-61804-055-8

For the frequency of the voltage waveform approaching infinity, $\Omega \to \infty$, it is possible to verify the following well-known facts from the above model: $\varphi(t) \to \varphi_{OP} \to \varphi_0$, or $\tilde{\varphi}(t) \to 0$, $q(t) \to q_{OP}$, or $\tilde{q}(t) \to 0$. In other words, the sweeping of the operating point along the CR dies away, and this point is fixed in the position $[\varphi_{OP}, q_{OP}]$, or $[\varphi_0, \tilde{q}(\varphi_0)]$. The memristance is then constant, and the memristor behaves as a linear resistor.

All the higher harmonic components of the current waveform, with the exception of the fundamental harmonic, disappear. The fundamental harmonic is then (see Eqs (18), (12), and (6))

$$i_1 = \tilde{g}_1 V = V \sum_{i=1}^{\infty} g_i i \varphi_0^{i-1} = G_M(\varphi_0) V . \qquad (19)$$

For $\Omega \to \infty$, the PHL in the *i-v* coordinates collapses to a line segment, passing through the origin, with the slope corresponding to the memductance for the initial flux φ_0.

4 Conclusions

The analytical method of Fourier analysis of current response of the general flux-controlled memristor, modeled by constitutive relation (1), to sine-wave voltage, is described. It is shown that the Fourier series of the memristor current can contain only sine-type terms and no DC component. That is why the hysteretic loop of each ideal memristor in the *i-v* coordinates must exhibit "pinched" and "odd-symmetry" attributes.

It also follows from the analysis that if the ideal memristor is excited from a voltage source which provides periodical signal with zero DC component, the memristor is passing immediately, without any transients, to the periodical steady state. This is because the flux, i.e. a state variable, which determines the position of the operating point at the CR curve and thus also the value of memconductance, comes after one repeating period back to its initial value.

Acknowledgments

This work has been supported by the Czech Science Foundation under grant No P102/10/1614, by the project CZ.1.07/2.3.00/20.0007 WICOMT of the operational program Education for competitiveness, and Project for the development of K217 Department, UD Brno – Modern electrical elements and systems.

References:

[1] Pershin, Y. V., Di Ventra, M. Memory effects in complex materials and nanoscale systems. *Advances in Physics*, vol. 60, 2011, pp. 145-227.

[2] Yang, J. J., Pickett, M. D., Li, X., Ohlberg, D. A. A., Stewart, D. R., and Williams, R. S. "Memristive switching mechanism for metal/oxide/metal nanodevices," *Nature Nanotechnology*, vol. 3, pp. 429-433, 2008.

[3] Lehtonen, E., Laiho, M. CNN Using Memristors for Neighborhood Connections. In *Proc. Cellular Nanoscale Networks and Their Applications* (CNNA), 2010, pp. 1-4.

[4] Pino, R. E. et al. Compact Method for Modeling and Simulation of memristor Devices. In *Proc. IEEE/ACM Int. Symp. Nanoscale Architectures* (NANOARCH), 2010, pp. 1-4.

[5] Williams, S. Finding the Missing Memristor. *IEEE CPMT Chapter*, Santa Clara Valley, February 11, 2009.

[6] Miller, K. Fabrication and modeling of thin-film anodic titania memristors. The MSc. Thesis, Iowa State University, Ames, Iowa, 2010.

[7] Chua, L. O. Resistance switching memories are memristors. *Applied Physics A, Materials Science & Processing*, 2011, Open Access at Springerlink.com, DOI 10.1007/s00339-011-6264-9.

[8] Chua, L.O., Kang, S.M. Memristive Devices and Systems. *Proc. of the IEEE*, vol. 64, no. 2, 1976, pp. 209-223.

[9] Miller, K. Fabrication and modeling of thin-film anodic titania memristors. The MSc. Thesis, Iowa State University, Ames, Iowa, 2010.

[10] Strukov, D. B. et al. The missing memristor found. *Nature*, 1 May 2008, pp. 80-83.

[11] Biolek, Z., Biolek, D., Biolkova, V. SPICE model of memristor with nonlinear dopant drift. *Radioengineering*, vol. 18, no. 2, Part II, 2009, pp. 210-214.

[12] Biolek, D., Biolek, Z., Biolkova, V. SPICE Modeling of Memristive, Memcapacitative and Meminductive Systems. In *Proc. of ECCTD '09, European Conference on Circuit Theory and Design*, August 23-27, 2009, Antalya, Turkey, pp. 249-252.

[13] Radwan, A.G., Zidan, M.A., Salama, K.N. On the mathematical modeling of memristors. In *Proc. 22th Int. Conf. on Microelectronics* (ICM 2010), Cairo, Egypt, 2010, pp. 284-287.

[14] Georgiou, P. S. et al. Quantitative measure of hysteresis for Bernoulli memristors. *arXiv*: 1011.0060v2 [cond-mat.mes-hall] 8 Nov 2010.

[15] Chua, L. O. Memristor–the missing circuit element. *IEEE Trans. Circ. Theory*, vol. CT-18, no. 5, 1971.

[16] Di Ventra, M., Pershin, Y. V. Practical Approach to Programmable Analog Circuits With Memristors. *IEEE Trans. on Circ. Syst. I: Regular Papers*, vol. 57, no. 8, 2010, pp. 1857-1864.